Can the human lumbar posterior columns be stimulated by transcutaneous spinal cord stimulation? A modeling study.

Running head: Modeling transcutaneous posterior columns stimulation

The definitive version is available at www.blackwell-synergy.com

Artificial Organs 35(3):257-62. DOI:10.1111/j.1525-1594.2011.01213.x

Simon M. Danner[1], Frank Rattay[1], Josef Ladenbauer[2], Ursula S. Hofstoetter[1,3], Karen Minassian[1,3]

[1] Institute for Analysis and Scientific Computing, Vienna University of Technology, Vienna, Austria

[2] Department of Software Engineering and Theoretical Computer Science, Technische Universität Berlin, Germany

[3] Center of Biomedical Engineering and Physics, Medical University of Vienna, Vienna, Austria

Author's Address

Karen Minassian

Institute for Analysis and Scientific Computing, Vienna University of Technology

Wiedner Hauptstraße 8-10/101

A-1040 Vienna, Austria

karen.minassian@gmail.com

Abstract

Stimulation of different spinal cord segments in humans is a widely developed clinical practice for modification of pain, altered sensation and movement. The human lumbar cord has become a target for modification of motor control by epidural and more recently by transcutaneous spinal cord stimulation. Posterior columns of the lumbar spinal cord represent a vertical system of axons and when activated can add other inputs to the motor control of the spinal cord than stimulated posterior roots. We used a detailed three-dimensional volume conductor model of the torso and the McIntyre-Richard-Grill axon model to calculate the thresholds of axons within the posterior columns in response to transcutaneous lumbar spinal cord stimulation. Superficially located large diameter posterior column fibers with multiple collaterals have a threshold of 45.4 V, three times higher than posterior root fibers (14.1 V). With the stimulation strength needed to activate posterior column axons, posterior root fibers of large and small diameters as well as anterior root fibers are co-activated. The reported results inform on these threshold differences, when stimulation is applied to the posterior structures of the lumbar cord at intensities above the threshold of large-diameter posterior root fibers.

Key words: Computer modeling, transcutaneous spinal cord stimulation, human, posterior columns

Introduction

The successful demonstration that epidural electrical stimulation of posterior spinal cord structures can suppress pain (1), led to a widely spread clinical practice of spinal cord stimulation (SCS) to modify the severity of perception of nociceptive and neuropathic pain. Clinical practice of SCS has been extensively reviewed (2,3,4,5). SCS for pain control has generally been applied to the thoracic spinal cord. Other spinal cord segments have been also targeted, like cervical segments for lungs bronchial tree dilatation, lower cervical and upper thoracic spinal cord segments to control pain in angina pectoris, sacral segments to augment bladder functions and lumbar segments for spasticity control (6,7). Furthermore, the human lumbar spinal cord has been shown to generate standing- and stepping-like movements after complete chronic, posttraumatic spinal cord injury when activated by tonic epidural stimulation (8,9). Recently, a method of transcutaneous spinal cord stimulation (tSCS) was described (10). Its potential for applications in neurophysiological studies (11) and in facilitation of treadmill stepping in spinal cord injured subjects (12, 13) was explored.

The purpose of the present study was to calculate under what conditions the system of parallel ascending axons within the posterior columns of the human lumbar spinal cord can be activated by tSCS. We will relate the findings to thresholds of posterior and anterior root fibers (14) that are conveying sensory inputs to and motor outputs from the lumbar spinal cord.

Information on the calculated thresholds for those three systems of the lumbar cord is significant for research designs of sensory-motor integration mechanisms of the human lumbar cord and for neurophysiological monitoring of lumbar spinal cord functions with intact and impaired connectivity with supraspinal structures. Moreover

this knowledge is essential for the development of new neurophysiological interventions to augment spinal cord motor control in paralyzed people (12,13).

Methods

A two-step method including a volume conductor and an axon model was applied (15). The volume conductor model was used to calculate the electrical potential generated by tSCS and to evaluate the potential distributions along the trajectories of the target fibers. Subsequently, the excitation process was simulated with the McIntyre-Richardson-Grill (MRG) axon model.

Anatomy

Three different fiber classes, posterior column, posterior root and anterior root fibers, were studied (see 1, 2, 4 in Fig. 1a). Lumbosacral root fibers have substantial curvatures at spinal cord and spinal canal entry and exit and are otherwise comparatively straight (16). Largest Ia afferent fibers within the posterior roots have a diameter of 20 µm (17,18). Here, 7 posterior and anterior root fibers, with diameters of 16 µm and 14 µm, respectively, and different entry and exit levels into and from the spinal cord (Fig. 1c), were simulated to account for the activation of a set of fibers. The diameters of the lowest threshold posterior and anterior root fibers were varied in 0.1 µm steps to match the lowest threshold of the posterior column fiber.

The posterior column fibers are vertical axons within the white matter with several perpendicular collaterals entering the gray matter (19,20). A mean of 0.5% of the fibers in the superficial 300 µm of the posterior column have a diameter larger than 10.7 µm (21). Here, we assumed a posterior column-fiber diameter of 11.5 µm with a collateral diameter of 5.7 µm and varied the position of the main axon (depth within the white matter, distance from the midsagittal plane; Fig. 1d).

Volume conductor model

A detailed three-dimensional volume conductor model, including the spinal cord, the vertebral column and other anatomical structures, was used (Fig. 1). Conductivity values [S/m] were: cerebrospinal fluid: 1.7, epidural fat: 0.04, white matter: 0.083 (transversal) and 0.6 (longitudinal), gray matter: 0.23, vertebral disc: 0.6, vertebral bone: 0.02, muscle: 0.08 (transversal) and 0.5 (longitudinal), fat: 0.04, skin: 0.0025, general thorax: 0.25, and electrode: 0.01. These values were adopted from a previous modeling study of tSCS (12). Due to the symmetry of the model, only one side separated by the midsagittal plane was simulated. Neumann boundary conditions were used for the external surface of the skin, the midsagittal symmetry plane and the bottom and top surfaces of the model. For the electrodes Dirichlet boundary conditions were used. The steady-state solution was calculated and evaluated along the target fiber trajectories with COMSOL Multiphysics 3.5 (COMSOL Inc., Burlington, MA).

Axon model

The MRG axon model was re-implemented with MATLAB 2010a (The Mathworks Inc., Natick, MA) to allow for a convenient input of arbitrary extracellular potentials (22). It was verified against the standard implementation with a series of tests with intra- and extracellular stimulation. Equations underlying the re-implementation not described in the original publication are presented below (22). The equation for all nodal compartments is given by

$$\frac{dV_m}{dt} = -(I_{ion} + g_{lk} \cdot (V_m - E_{lk}) + I_{ax}) / c_{mem} \quad (1)$$

where I_{ion} is the sum of the ion currents as specified in (22), V_m is the transmembrane voltage, E_{lk} the leakage resting potential, g_{lk} the leakage conductance, I_{ax} the axonal current (see eq. 4) and c_{mem} the capacitance of the membrane.

The myelin sheath of the internodes is modeled as a double cable structure, where current can flow in the periaxonal space between the axon membrane and the myelin sheath. The axonal compartment is modeled according to eq. 2 and the periaxonal compartment according to eq. 3, where g_{mem} is the membrane conductance, g_{my} the myelin conductance, V_p the potential difference between periaxonal space and the outside of the myelin sheath, E_{pas} the reversal potential of the membrane, c_{my} the myelin capacitance, I_{px} the periaxonal current resulting from neighboring compartments, E_i is the intracellular potential measured against the ground, E_p is the periaxonal potential measured against the ground, R^i is the axonal resistance, R^p the resistance along the periaxonal space and the index k stands for the compartment number.

$$\frac{dV_m}{dt} = -(g_{mem} \cdot (V_m - E_{pas}) + I_{ax}) / c_{mem} \tag{2}$$

$$\frac{dV_p}{dt} = -(g_{my} \cdot V_p + I_{ax} + I_{px}) / c_{my} \tag{3}$$

$$I_{ax} = \frac{E^i_k - E^i_{k+1}}{(R^i_k - R^i_{k+1})/2} + \frac{E^i_k - E^i_{k-1}}{(R^i_k - R^i_{k-1})/2} \tag{4}$$

$$I_{px} = \frac{E^p_k - E^p_{k+1}}{(R^p_k - R^p_{k+1})/2} + \frac{E^p_k - E^p_{k-1}}{(R^p_k - R^p_{k-1})/2} \tag{5}$$

To incorporate the effect of extracellular stimulation, an equivalent injected intracellular current (I_{int}, eq. 6) is added to every intracellular compartment (23,24). The extracellular potential V^e directly outside the compartment follows from the volume conductor model.

$$I_{\text{int}} = \frac{V^e_k - V^e_{k+1}}{(R^i_k - R^i_{k+1})/2} + \frac{V^e_k - V^e_{k-1}}{(R^i_k - R^i_{k-1})/2} \tag{6}$$

For fibers with branches, the branching node is modeled by extending the intra axonal current (I_{ax}) and the equivalent intracellular current (I_{int}) of the extracellular potential as:

$$I_{ax} = \frac{E_k^i - E_{k+1}^i}{(R_k^i - R_{k+1}^i)/2} + \frac{E_k^i - E_{k-1}^i}{(R_k^i - R_{k-1}^i)/2} + \frac{E_k^i - E_{coll,1}^i}{(R_k^i - R_{coll,1}^i)/2} \quad (7)$$

$$I_{int} = \frac{V_k^e - V_{k+1}^e}{(R_k^i - R_{k+1}^i)/2} + \frac{V_k^e - V_{k-1}^e}{(R_k^i - R_{k-1}^i)/2} + \frac{V_k^e - V_{coll,1}^e}{(R_k^i - R_{coll,1}^i)/2} \quad (8)$$

where the subscript ‘coll,1’ denotes the first compartment of the collateral (25). Adaptation of the periaxonal current I_{px} is not necessary because the branching always occurs at a node of Ranvier (26), which is not covered with myelin. Parameters for different axon diameters were linearly interpolated.

Stimulation configuration

Two 5 cm-diameter electrodes placed over the T11–T12 vertebral processes on each side of the spine were used for stimulation together with large indifferent electrodes over the abdomen (Fig. 1b, for details see 10,11). All simulations were conducted with rectangular 1 ms-pulses. Excitation thresholds determined by a binary search with a final step of 0.1 V. All thresholds, if not noted otherwise, were calculated with the paravertebral surface electrodes being at negative potential. Since shifting the node positions in steps of a tenth of the node-to-node distance of one representative fiber of each type resulted only in a maximum variation of 1.43% of the excitation thresholds, the influence of node position on threshold values was not studied in detail.

Results

Posterior column fiber position and diameter

The relation between excitation threshold and position of the straight posterior column fibers, without collaterals, was investigated with variations in anteropostero and mediolateral direction. The fiber at the most superficial (50 µm depth) and medial position within the white matter had the lowest threshold of 67.4 V. Thresholds increased for any variation of the position, but considerably more for anterior than lateral locations. The intensity required to recruit the deepest fiber in the midsagittal plane of the posterior columns (2mm depth) increased by 54.0% to 103.8 V. On the other hand, an increase of stimulus intensity by only 4.5% to 70.4 V was required to activate superficially located fibers at the most lateral position (2 mm from midline) in the posterior columns. Figure 2 depicts the dependence of the excitation threshold on the fiber position within the posterior columns, with some of the evaluated locations illustrated in Fig. 1d.

Effects of collaterals on posterior column fiber threshold

Collaterals were introduced for the posterior column fiber located most superficially in the midsagittal plane of the white matter. First, a single collateral was attached to the node of Ranvier that was the action potential initiation site of the simple, straight fiber. This branching reduced the threshold of the straight fiber from 67.4 V to 59.6 V. Five additional collaterals in superior as well as in inferior direction with a spacing of one internode (1.25 mm) further reduced the threshold to 45.4 V.

Excitation of posterior column fibers compared to posterior and anterior root fibers

The potential distributions along the different fiber classes had characteristic features. The external potential along the posterior root fibers varied strongest at two sites, at their entry into the vertebral canal and into the spinal cord. Anterior roots yielded strong potential variations at their exits from the spinal cord and the vertebral canal. At the entries into the spinal cord, the potential distribution changes along posterior

root fibers were inverse to those of the corresponding anterior root fibers at their spinal cord exits. At more distant sites, the potential distributions of anterior and posterior root fibers of the same spinal cord segment were alike. The external potential distribution along the posterior column fiber had no sudden changes.

Representative potential distributions and activating functions (providing a first approximation of the initial effects of external stimulation) are illustrated for selected fibers for cathodic stimulation at 1 V in Fig. 3. Posterior and anterior root fibers had their entries into and exits from the spinal cord at the center of the stimulation electrodes. Note that the potential values along the fibers varied within a small range of 0.02 V. The excitation thresholds for these fibers were 17.6 V, 51.7 V and 67.4 V for the posterior root, anterior root and posterior column fibers, respectively. The positive peaks of the activating functions indicated the stimulation sites of the different fibers marked by arrows in Fig. 3a,c. The posterior root fiber was activated at its transition from the cerebrospinal fluid to the white matter, the anterior root fiber at its exit from the vertebral canal and the posterior column fiber close to the central level of the stimulation electrode, at their respective excitation thresholds. Threshold values for all simulated posterior (Ø 16 µm) and anterior roots (Ø 14 µm) are listed in Table 1. Lowest values were 14.1 V and 22.6 V, respectively. At the lowest stimulus intensity that activated posterior column fibers (45.4 V) posterior and anterior root fibers with diameters as small as 6.5 µm and 8.4 µm, respectively, were recruited.

Discussion

The present modeling study investigated the effect of tSCS on posterior column fibers. Excitation thresholds of superficially and medially located posterior column fibers with multiple collaterals, calculated with the MRG axon model, were three times higher than those of large-diameter posterior root fibers. At the lowest excitation

threshold of a posterior column fiber, a large set of root fibers with a variety of diameters and associated with different spinal cord segments were concomitantly activated.

The myelinated axon was shown to be the most excitable part of the nervous system (27) and the MRG model was demonstrated to realistically reproduce excitation thresholds in case of transcutaneous stimulation (28). Although the thresholds of the most excitable posterior column fibers are rather high, a slight increase beyond threshold additionally recruits a set of fibers at different locations within the posterior columns (Fig. 2) originating from multiple spinal cord segments (19). Regarding segmental effects, posterior column stimulation can thus be expected to be nonspecific. While with tSCS the deepest fibers within the posterior columns require an increase by half the threshold of the superficially located ones to be recruited, it should be noted that the effect of epidural SCS is restricted to a superficial layer only (threshold increase by 150% at a depth of 0.7 mm; 29). Here, the presence of one collateral reduced the threshold to 88% and of eleven collaterals to 67%, respectively. In epidural stimulation of the thoracic spinal cord, thresholds of posterior columns with 11 collaterals were within the range of 50–60% (20). At the threshold of posterior column stimulation, anterior and posterior root fibers of different segments (Table 1) and of smaller diameters are activated simultaneously.

When applying tSCS it can be expected that the activation order when increasing stimulation intensity is first posterior root fibers (identifiable by elicitation of posterior root-muscle reflexes; 10,30), second anterior root fibers (identifiable by M waves; 10) and third posterior column fibers. Posterior column fibers cannot be stimulated with a single pulse without concomitant activation of root fibers. The directly electrically stimulated neuronal structures represent the input pathways that transsynaptically

activate spinal mechanisms. Hence, their identification is essential for understanding the neurophysiology underlying tSCS as well as advancing intervention methods based on the conducting and processing capabilities of the human lumbar cord.

Acknowledgements

This study was supported by the Austrian Science Fund (FWF), project no. L512-N13. We would like to thank Em. Prof. Dr. Milan R. Dimitirijevic, Department of Physical Medicine and Rehabilitation, Baylor College of Medicine, Houston, TX, USA for his comments and discussions during the development of this manuscript.

References

1. Shealy CN, Mortimer JT, Reswick J. Electrical inhibition of pain by stimulation of the dorsal column: Preliminary clinical report. Anesth Analg 1967;46:489-491.
2. Barolat G. Spinal cord stimulation for chronic pain management. Arch Med Res 2000;31:258-262.
3. Simpson B, Meyerson B, Linderoth B. Spinal cord and brain stimulation. In: McMahon S, Koltzburg M, editors. Textbook of Pain, 5th edn. Amsterdam: Elsevier, 2005.
4. Lee A, Pititsis J. Spinal cord stimulation: indications and outcomes. Neurosurg Focus 2006;21:1-6.
5. Lozano, AM, Gildenberg PL, Tasker RR, editors. Textbook of stereotactic and functional neurosurgery, 2nd edn. Berlin-Heidelberg: Springer; 2009.
6. Linderoth B, Foreman RD, Meyerson BA. Mechanisms of action of spinal cord stimulation. In: Lozano, AM, Gildenberg PL, Tasker RR, editors. Textbook of stereotactic and functional neurosurgery, 2nd edn. Berlin-Heidelberg: Springer; 2009.
7. Dimitrijevic MR. Chronic spinal cord stimulation for spasticity. In: Gildenberg PL, Tasker RR, editors. Textbook of stereotactic and functional neursurgery, New York: McGraw-Hill, 1998.
8. Dimitrijevic MR, Gerasimenko Y, Pinter MM. Evidence for a spinal central pattern generator in humans. Ann N Y Acad Sci. 1998;860:360-376.
9. Minassian K, Persy I, Rattay F, Pinter MM, Kern H, Dimitrijevic MR. Human lumbar cord circuitries can be activated by extrinsic tonic input to generate locomotor-like activity. Hum Mov Sci 2007;26:275-295.

10. Minassian K, Persy I, Rattay F, Dimitrijevic MR, Hofer C, Kern H. Posterior root-muscle reflexes elicited by transcutaneous stimulation of the human lumbosacral cord. Muscle and Nerve 2007;35:327-336.

11. Hofstoetter US, Minassian K, Hofer C, Mayr W, Rattay F, Dimitrijevic MR. Modification of reflex responses to lumbar posterior root stimulation by motor tasks in healthy subjects. Artificial Organs 2008;32:644-648.

12. Minassian K, Hofstoetter U, Tansey K, Rattay F, Mayr W, Dimitrijevic MR. Transcutaneous stimulation of the human lumbar spinal cord: Facilitating locomotor output in spinal cord injury. Program No.286.19. Neuroscience Meeting Planner. San Diego, CA: Society for Neuroscience, 2010. Online.

13. Minassian K, Hofstoetter US, Tansey K, Rattay F, Mayr W, Dimitrijevic MR. Neurophysiology of the human lumbar locomotor pattern generator. Artificial Organs 2010;34:A41.

14. Ladenbauer J, Minassian K, Hofstoetter, US, Dimitrijevic MR, Rattay F. Stimulation of the human lumbar spinal cord with implanted and surface electrodes: A computer simulation study. IEEE Trans Neural Syst Rehab Eng. doi: 10.1109/TNSRE.2010.2054112

15. Holsheimer J. Computer modelling of spinal cord stimulation and its contribution to therapeutic efficacy. Spinal Cord 1998;36:531-540.

16. Kayalioglu G. The spinal nerves. In: Watson C, Paxinos G, Kayalioglu G, editors. The spinal cord. London: Elsevier; 2009.

17. Lloyd DCP. Neuron patterns controlling transmission of ipsilateral hind limb reflexes in cat. Journal of Neurophysiology 1943;6:293-315.

18. Brodal P, Rinvik E. The somatic afferent pathway. In: Brodal A editor. Neurological anatomy in relation to clinical medicine. New York: Oxford University Press; 1981.

19. Smith MC, Deacon P. Topographical anatomy of the posterior columns of the spinal cord in man. Brain 1984;107:671-698.

20. Struijk JJ, Holsheimer J, van der Heide GG, Boom BHK. Recruitment of dorsal column fibers in spinal cord stimulation: influence of collateral branching. IEEE Trans Biomed Eng 1992;32:903-912.

21. Feirabend HKP, Choufoer H, Ploeger S, Hosleimer J, van Gool JD. Morphometry of human superficial dorsal and dorsolateral column fibers: Siginificance to spinal cord stimulation. Brain 2002;125:1137-1149.

22. McIntyre CC, Richardson AG, Grill WM. Modeling the excitability of mammalian nerve fibers: Influence of after potentials on the recovery cycle. Journal of Neurophysiology 2002;87:995-1006.

23. Warman EN, Grill WM, Durand D. Modeling the effects of electric fields on nerve fibers: Determination of excitation thresholds. IEEE Trans Biomed Eng 1992;32:1244-1254.

24. Grill WM. Modeling the effects of electric fields on nerve fibers: Influence of tissue electrical properties. IEEE Trans Biomed Eng 1999;46:918-928.

25. Dayan P, Abbott LF. Theoretical neuroscience: Computational and mathematical modeling of neural systems. Cambridge, MSS: MIT-Press; 2001.

26. Stoney SD. Limitations on impulse conduction at the branch point of afferent axons in frog dorsal root ganglion. Exp Brain Res 1990;80:512-524.

27. Ranck JB Jr. Which elements are excited in electrical stimulation of mammalian central nervous system: a review. Brain Res 1975;98:417-440.

28. Kuhn A, Keller T, Lawrence M, Morari M. A model for transcutaneous current stimulation: Simulations and experiements. Med Biol Eng Comput 2009;47:279-289.

29. Holsheimer J. Which neuronal elements are activated directly by spinal cord stimulation. Neuromodulation 2002;5:25-31.

30. Minassian K, Jilge B, Rattay F, Pinter MM, Binder H, Gerstenbrand F, Dimitrijevic MR. Stepping-like movements in humans with complete spinal cord injury induced by epidural stimulation of the lumbar cord: Electromyographic study of compound muscle action potentials. Spinal Cord 2004;42:401-416.

Figures

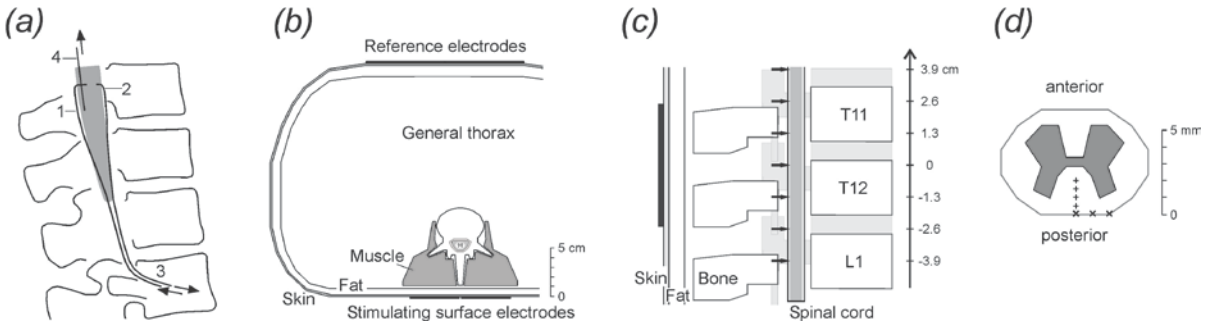

Figure 1.

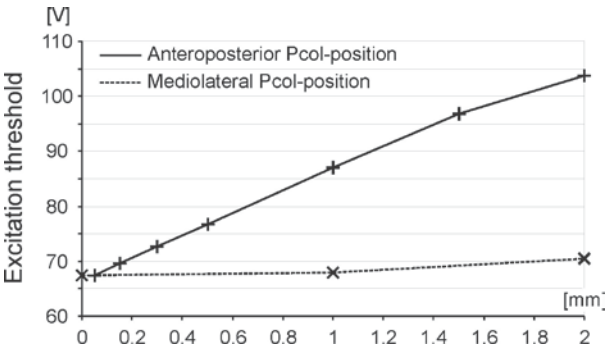

Figure 2.

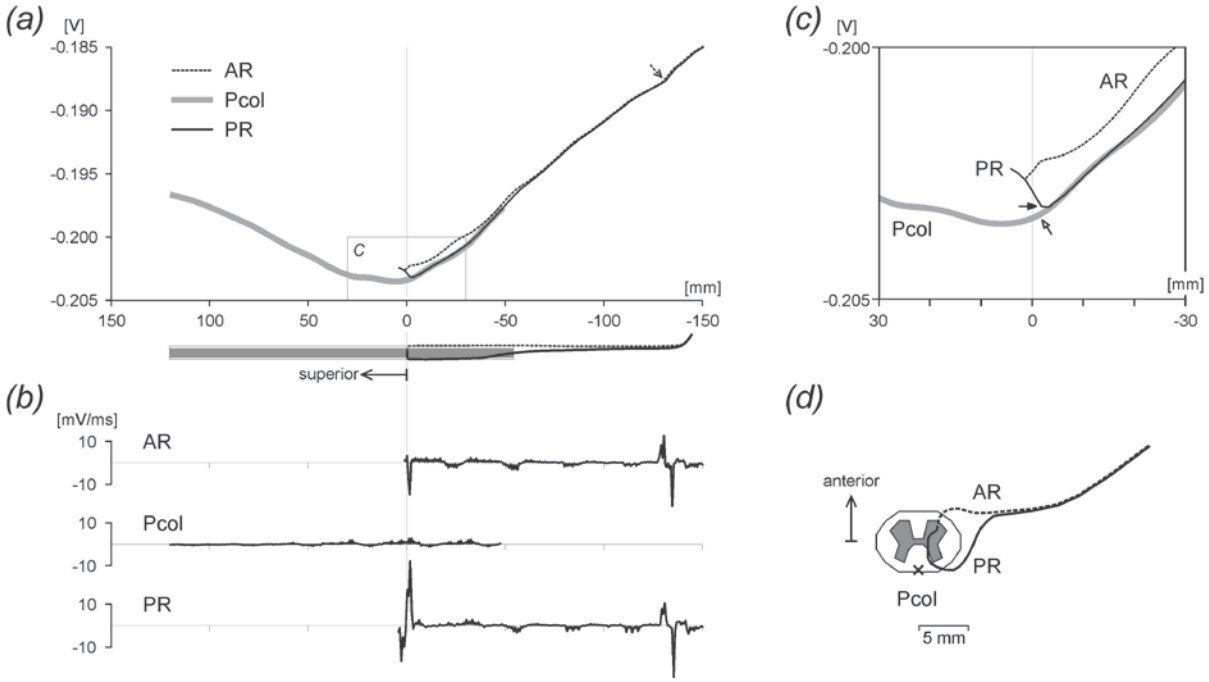

Figure 3.

Tables

	posterior root		*anterior root*	
d[1]	neg	pos	neg	pos
3.9	20.1	50.0	23.2	22.6
2.6	26.1	51.5	28.9	37.1
1.3	29.5	49.5	37.1	51.4
0	17.6	65.0	51.7	67.9
-1.3	21.5	87.1	72.2	68.5
-2.6	14.1	110.9	82.4	67.6
-3.9	14.4	114.1	33.9	70.9

[1] *d* denotes the vertical distance in cm from the entry point of the root fiber into the spinal cord from the center of the stimulation electrode, cf. Fig. 1c.

Table 1.

Legends

Figure 1. Information on the volume conductor model and positions of simulated fibers. (a) Sketch of posterior roots (1) and anterior roots (2) joining to form the spinal nerves (3), and of the posterior columns (4) in relation to the spinal cord and the vertebrae. (b) Transverse section of the model with compartments of different electrical conductivities as well as surface electrodes. (c) Entry (and exit) levels of simulated posterior and anterior root fibers, respectively, marked by arrows. Reference center of the inferior-to-superior axis is given by the center of the stimulation electrode. (d) Section of the spinal cord consisting of white and grey matter with some of the positions of simulated posterior column fibers indicated.

Figure 2. Dependence of the excitation threshold of posterior column fibers on the fiber position. Anteroposterior depths within the midsagittal plane studied were 50, 150, 300, 500, 1000, 1500 and 2000 μm and mediolateral positions were 0, 1000 and 2000 μm at 50 μm depth within the white matter, cf. figure 1(d). The posterior column fibers were modeled as straight fibers of 11.5 μm diameter.

Figure 3. Stimulation effect evaluated along sensory structures and motor fibers. (a) Extracellular potential V^e along selected target fibers generated by transcutaneous spinal cord stimulation at -1 V. Posterior root (PR) and anterior root (AR) fibers enter and exit the spinal cord at the central level of the stimulation electrode, respectively. The posterior column (Pcol) fiber is located medially and superficially in the white matter. The abscissa is the distance along the fiber trajectories from the level of the center of the stimulation electrode. The dashed arrow shows the site of action potential initiation of the AR fiber. Anatomical relations of the PR and AR fiber are illustrated below the abscissa. (b) Activating functions corresponding to cases in (a). (c) Enlarged view of the box in (a). Arrows indicate the lowest threshold sites of the

PR and Pcol fiber, respectively. (d) Top view of the trajectories of the AR and PR fibers and of the simulated Pcol fiber location (x).

Table 1. Excitation thresholds of posterior (16 μm diameter) and anterior root (14 μm diameter) fibers for negative and positive single pulse stimulation.